Available online at www.sciencedirect.com

ScienceDirect

Energy Procedia 55 (2014) 797 – 804

Energy Procedia

4th International Conference on Silicon Photovoltaics, SiliconPV 2014

Investigations on the passivation mechanism of AlN:H and AlN:H-SiN:H stacks

Georg Krugel[a,]*, Franziska Jenkner[b], Anamaria Moldovan[b], Winfried Wolke[b], Jochen Rentsch[b], Ralf Preu[b]

[a]Fraunhofer Institute for Mechanics of Materials, Wöhlerstr. 11, 79108 Freiburg, Germany
[b]Fraunhofer Institute for Solar Energy Systems, Heidenhofstr. 2, 79110 Freiburg, Germany

Abstract

In this paper, the properties of hydrogenated aluminum nitride layers (AlN:H) as an excellent passivation layer of silicon surfaces are examined. The structural and chemical properties of the AlN:H bulk are analyzed using a great variety of measurements techniques such as GI-XRD, FTIR, SEM, HR-TEM, corona charging and a thickness dependent measurements of the surface passivation. A model for the formation of negative fixed charges at the interface to silicon is presented based on the charge state of ionized point defects in AlN.

Additionally, stacks of AlN:H and SiN_x:H are introduced into silicon photovoltaics and their combination with two different types of thin low temperature silicon oxide layers is studied. Excellent passivation results are presented for highly doped p-type silicon and highly doped n-type silicon using the previous described stacks. Emitter saturation current densities of textured samples show, that 75 Ω/sq. phosphorous emitter can be passivated as efficient as with the typically used SiN_x:H allowing maximum open circuit voltages of 657 mV. This is supported by measurement of cell parameters of p-type solar cells using these stacks as a combined anti-reflective coating and passivation layer. Furthermore, the passivation level reached for high efficiency 70 Ω/sq. boron emitters is nearly as high as with excellent passivating PECVD Al_2O_3/SiN_x stacks. Emitter saturation current densities down to 61 fA/cm^2 are presented corresponding to a maximum open circuit voltage of 696 mV. This indicates that the invented stacks containing AlN:H can also be applied as combined anti-reflective coating and passivation layers in n-type cells.

© 2014 The Authors. Published by Elsevier Ltd. This is an open access article under the CC BY-NC-ND license (http://creativecommons.org/licenses/by-nc-nd/3.0/).
Peer-review under responsibility of the scientific committee of the SiliconPV 2014 conference

Keywords: passivation; aluminum nitride; hydrogen

* Corresponding author. Tel.: +49-761-5142-293; fax: +49-761-5142-510.
E-mail address: georg.krugel@iwm.fraunhofer.de

1876-6102 © 2014 The Authors. Published by Elsevier Ltd. This is an open access article under the CC BY-NC-ND license (http://creativecommons.org/licenses/by-nc-nd/3.0/).
Peer-review under responsibility of the scientific committee of the SiliconPV 2014 conference
doi:10.1016/j.egypro.2014.08.062

1. Introduction

Thin layers of hydrogenated aluminum nitride have recently been introduced to silicon photovoltaic as an alternative to silicon oxide, silicon nitride and aluminum oxide [1]. Beside ideal properties as anti-reflective coating this material also allows excellent passivation of shiny etched surfaces of FZ silicon wafers, for lowly doped silicon [1] as well as for highly doped silicon [2]. The reported interface defect densities are in the order of $5 \times 10^{10}\,eV^{-1}\,cm^{-2}$ in combination with a fixed negative charge density of $1 \times 10^{12}\,cm^{-2}$. However, a detailed understanding of the passivation mechanism has not been presented so far. This will be discussed in the first part of the paper. The second part focuses on the application of AlN:H and AlN:H containing stacks for the passivation of highly doped silicon surfaces. In addition, results for symmetrical test structures and for PERC solar cells are presented.

2. Approach

Passivation layer of AlN:H are deposited with an inline sputter coater (ATON500 by Applied Materials) using an aluminum target with nitrogen and hydrogen as reactive gases. Further information can be found in [3] and [4]. These layers are combined with PECVD SiN_x:H capping layers (Roth & Rau). Additionally, the silicon surfaces are pre-conditioned with two different types of thin low temperature oxides. The first (wet chemical, oxide 1) oxide is formed by oxidation in concentrated HNO_3, the second (dry chemical, oxide 2) oxide originates during an exposure to an excimer UV lamp by oxidation with O_3. These two types of low temperature oxides are described extensively in [5].

3. Results and discussion

3.1. Structural properties

Scanning electron microscopy (SEM) is used to get an overview of the structural growth of the AlN:H layers. For this goal 1 µm of AlN:H is deposited on FZ silicon wafers and subsequently measured (see Fig. 1).

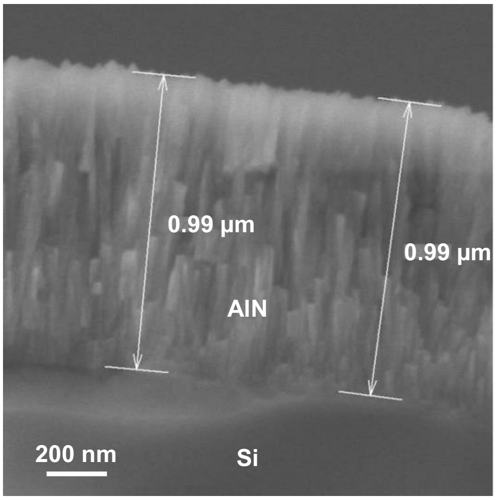

Fig. 1. Example of a SEM image of a 1 µm thick layer of sputtered AlN:H.

The growth of sputtered layers is very uniform with a variation in thickness lower than 3%. The structure exhibit a columnar growth which is typical for sputtered layers. The diameter of the columns is around 15-30 nm. Grazing incidence X-ray diffraction is used to get information about the crystallinity of these structures. The resulting diffraction pattern is shown in Fig. 2.

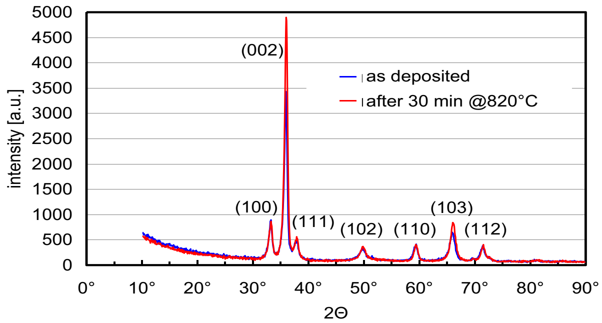

Fig. 2. GI-XRD spectrum (Bruker D8 Advance) of a 200 nm layer of AlN:H.

The detected peaks can easily be identified and assigned to different diffracting planes of AlN in the wurtzite crystal structure [6] [7]. The observed pattern reveals a polycrystalline growth. The dominating [002] orientation is typical for sputtered AlN layers and is also observed by Engelmark [7]. Using the Scherrer equation, it is possible to estimate the dimension of the crystallites [8]. Crystallite sizes of about 20 nm are obtained for the dominating peaks which matches the diameter of the columnar structures identified in SEM images (Fig. 1).

The atomic configuration directly at the interface is crucial for a better understanding of the passivation mechanism of the silicon surface. High resolution transmission electron microscopy exhibit that the AlN:H films grow in a polycrystalline configuration, even very close to the wafer surface (Fig. 3).

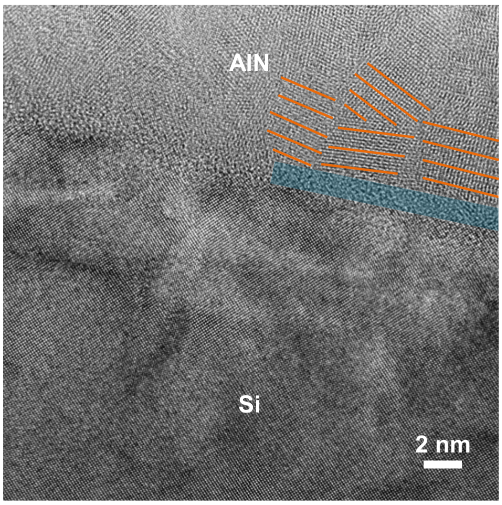

Fig. 3. High resolution TEM image of the region near to interface for a 30 nm thick layer of AlN:H after firing at 820°C for a few seconds. A thin wet-chemical oxide (approx. 1-2 nm, see above) has been deposited on the FZ silicon wafer prior to sputtering of the AlN:H layer. Some exemplary planes of the AlN:H are depicted as well.

The different crystallites are packed dense. This is in concordance with the also determined mass density of the sputtered AlN:H layers which is about 93 ± 2 % of the mass density of crystalline AlN in the wurtzite structure [9]. Drüsedau traces the high density of sputtered AlN layers back to a bombardment of energetic ions [10] [11]. The visible amorphous layer directly at the interface (Fig. 3) can be caused by the applied thin wet-chemical oxide. It can also be a combination of a thin amorphous layer of the oxide in combination with an amorphous growth of AlN:H in the first atomic layers. Such behaviour has been reported by Yong for sputtered AlN:H layers [12]. This cannot be decided without a doubt from this measurement.

The occurring chemical bonds are analyzed by FTIR (Fig. 4). The determined absorbance exhibits the expected peak at 667 cm^{-1} belonging to the TO mode of the Al-N bond [13]. Nevertheless, the missing peaks for Al-H bonds at 2110 cm^{-1} and 2200 cm^{-1} and the very low intensity for N-H bonds at 3000 and 3750 cm^{-1} indicate that only a very low fraction of hydrogen is bonded in the AlN:H layer.

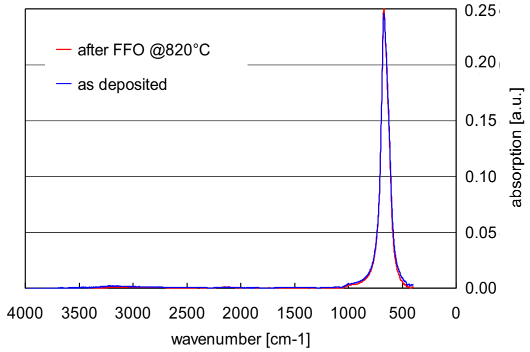

Fig. 4. FTIR spectrum of a 50 nm layer (Bruker IFS113V).

3.2. Analysis of interface parameters

3.2.1. Dependence from the layer thickness

Deeper insight into the passivation mechanism is obtained by a thickness variation (4 to 80 nm) of AlN:H as a passivation layer of 1 Ωcm p-type FZ silicon wafers. Contactless CV measurements are used to characterize the interface. With this method (COCOS, SDI Semilab) it is possible to determine the density of fixed charges at the interface Q_{fix} and the interface defect density D_{it} [14]. The effective lifetime (WCT-120, Sinton Instruments) is measured as well. Fig. 5 shows the determined parameters. Both characterization methods are carried out before and after a fast firing step with peak temperatures around 820°C for 1-2 seconds.

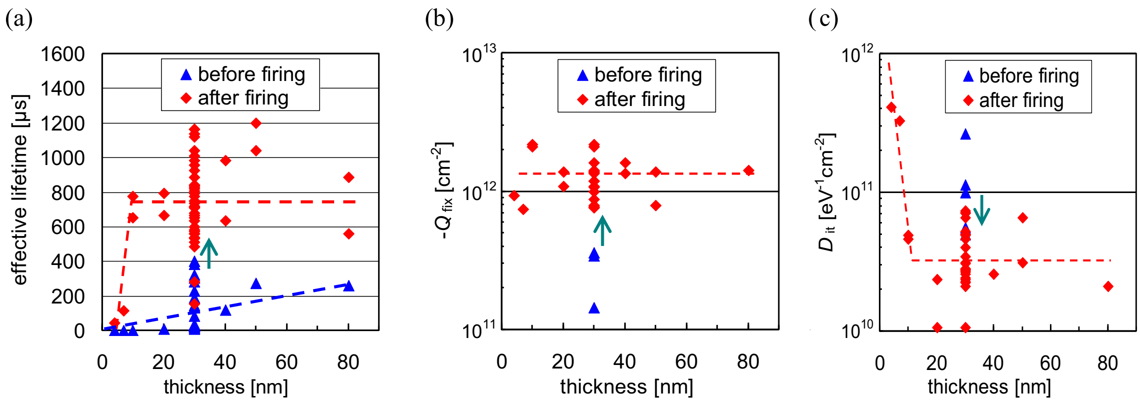

Fig. 5. (a) Effective Lifetime, (b) density of fixed charges at the interface and (c) interface defect density for AlN:H layers of different thickness. The influence of a short firing step is analyzed for a thickness of 30 nm. Lines are used to guide the eye. The layers are deposited on shiny etched 1 Ωcm p-type FZ wafers having a thin out-of-box interface oxide.

The activation of the passivation due to a high temperature step shown in Fig. 5 (a) step has been observed earlier [1]. The here presented results reveal that this activation is due to both, an increase of the density of fixed charges at the interface (Fig. 5 (b)) as well as an improved chemical passivation (Fig. 5 (c)). Furthermore, it can be seen that a layer thickness above 10 nm leads to a sufficient passivation of the Si (100) surface with lifetimes higher than 600 µs after firing. This corresponds to effective surface recombination velocities below 20 cm/s. The application of thinner layers has only a minor impact on the formation of the density of negative charges at the interface which are independent of the thickness around $-1\cdot10^{12}$ cm^{-2}. Apparently, the charge formation takes place directly at the interface, i.e. inside the first 4 nm of the AlN:H layer (see section 3.2.3). In contrast, the interface defect density shows an increase when reducing the layer thickness. A similar decrease in chemical passivation for thinner layers is also reported for Al_2O_3 where this is traced back to a reduced availability of hydrogen [15].

A model for the formation of the density of negative charges at the interface is presented below.

3.2.2. Dependence from pre-conditioning

More information about the passivation mechanism can be extracted from a variation of the pre-conditioning of the silicon surface directly before coating the Si (100) surface with AlN:H. Here, the two above described low temperature oxides are applied and additionally a combination of AlN:H in a stack with SiN_x:H is studied. The tested combinations of passivation layer stacks are summarized in Table 1 together with their corresponding interface parameters.

Table 1. Interface defect density and density of fixed charges at the interface determined for shiny etched 1 Ωcm p-type FZ wafers (Si (100) surface, after firing at 820°C for a few seconds).

Passivation layer	80nm AlN:H (after HF dip)	Oxide 1 + 80nm AlN:H	10nm AlN:H + 70nm SiN:H (after HF dip)	Oxide 1 + 10nm AlN:H + 70nm SiN:H	Oxide 2 + 10nm AlN:H + 70nm SiN:H
Q_{fix} [cm^{-2}]	$-3\cdot10^{11}$	$-5\cdot10^{11}$	$+5\cdot10^{10}$	$-3\cdot10^{11}$	$-3\cdot10^{11}$
D_{it}[eV^{-1}cm^{-2}]	$2\cdot10^{11}$	$5\cdot10^{10}$	$4\cdot10^{11}$	$5\cdot10^{10}$	$2\cdot10^{11}$

Comparing the corresponding layers it can be seen that thin oxides at the interface support the formation of negative fixed charges (see section 3.2.3). These oxides furthermore lead to a reduction of the interface defect density. A possible explanation is that the inserted thin oxide with its flexible bonds can reduce the density of defects at the interface between silicon and the AlN layer.

The application of a capping layer of SiN_x:H influences the resulting density of fixed charges (see Table 1). Their density is reduced for both cases, with and without thin oxide at the interface. This makes the presented stacks suitable to passivate both, highly doped n^+ and p^+ silicon.

3.2.3. Model of the charge formation at the interface

The formation of the fixed charges takes place directly at the interface within the first 4 nm of the AlN:H layer and is reinforced by the presence of a thin oxide and a high temperature firing step. This can be caused by a diffusion or transformation of the atomic configuration directly at the surface. Diffusion processes are analyzed here taking into account the charge state of ionized point-defects in crystalline aluminum nitride.

A first explanation for the formation is the coalescence of an aluminum vacancy (V_{Al}^-) and a nitrogen vacancy (V_N^+) inside the AlN (Fig. 6, Process A). Whereas the aluminum vacancy is preferably negatively charged the nitrogen vacancy is positively charged in AlN [16] [17] according to the ionic nature of the Al-N bond. Density functional theory calculation predict, that the combined vacancy $(V_{Al}\text{-}V_N)^-$ is negatively charged as well [16]. A formation of negative charges during a firing step can therefore be explained by this defect complex formation.

A diffusion of Al from the AlN into the thin interfacial oxide can furthermore explain the observed enhancement (see Table 1) when using a thin interface oxide (Fig. 6, Process B). Thereby, an aluminum vacancy is left inside the AlN layer, which is energetically favorable in a negatively charged charge state (V_{Al}^-) [16] [17]. Furthermore, a tetrahedrally coordinated Al inside silicon oxide can build up a net negative charge as well and is reported to be the reason for the negative charges of aluminum oxide layers [18]. The diffusion length of Al in silicon oxide is in the nanometer range making this process possible. These both processes can therefore explain the observed formation of a negative charge density during a high temperature firing step.

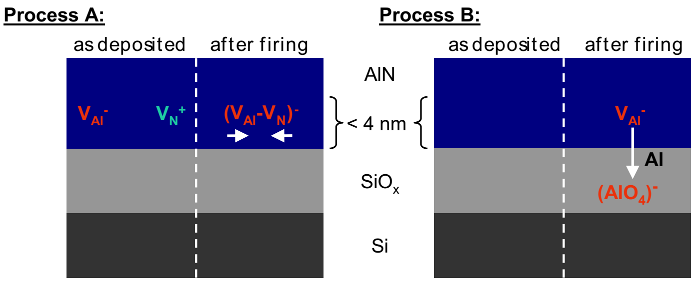

Fig. 6. Scheme of an AlN layer deposited on an oxidized silicon surface. The charge state of ionized point defect is used to explain the formation of negative charges inside the first nanometer during a short firing step at temperatures above 800°C (see text).

It has to be mentioned that also a reconstruction of the atomic configurations directly at the interface (i.e. the first atomic layers) could be responsible for the formation of the negative charges. However, no theoretical data are available for charge state of point defects in these complex surroundings.

3.3. Passivation of solar cell emitters

After this discussion of the passivation mechanism some results for AlN:H layers as a passivation layer for solar cell emitters are presented, first for symmetrical test structures and subsequently directly in solar cells.

3.3.1. Test structures

Five different stacks are investigated for the passivation of p^+ (boron, 70 Ω/sq.) and n^+ emitters (phosphorus, 75 Ω/sq). Therefore, textured symmetrical lifetime samples are fabricated using p-type FZ wafers (1 Ωcm) for the phosphorous emitter and n-type FZ wafers (1 Ωcm) for the boron emitter. The emitter saturation current density j_{0e} after a firing step at 820°C is calculated from QSSPC measurements [19] [20]. The results are shown in Fig. 7.

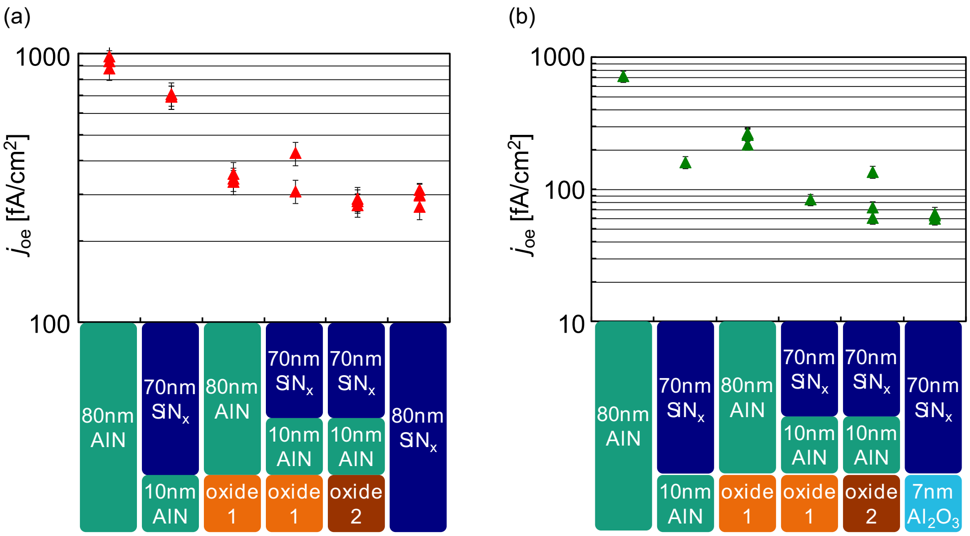

Fig. 7. Emitter saturation current density (a) for a 75 Ω/sq. phosphorus emitter and (b) for a 70 Ω/sq. boron emitter using different passivation stacks (both for a textured surface and after firing at 820°C).

It can be seen that j_{0e} is strongly affected by the chosen passivation stack. Both thin oxides at the interface as well as a SiN_x:H capping layer improve the passivation drastically. The improvement induced by the oxides is likely to be caused by the lower interface defect density shown in Table 1. The beneficial effect of the SiN_x:H capping layer is believed to be due to hydrogen diffusion which can passivate defects at the highly doped textured silicon surface. As a result of these effects, the same level of surface passivation can be achieved as in the case of the typically used SiN_x:H for a phosphorous emitter, whereas the passivation of boron emitters is nearly as efficient as with a predominantly applied stack of Al_2O_3 and SiN_x:H.

An upper limit for the open circuit voltage of solar cells can be calculated by using the one diode equation and neglecting recombination in the base. For the sample with the lowest j_{0e} maximum open circuit voltages $V_{oc,max}$ of 657 mV and 796 mV are obtained for the phosphorus and for the boron emitter respectively.

3.3.2. Application of AlN:H in solar cells

Additionally PERC solar cells based on 2 Ωcm p-type Cz silicon wafers (156'', industrial-like fabrication steps) are fabricated using some of these stacks (see Fig. 8) as an anti-reflective coating and passivation layer on the front. The rear is passivated using a stack of PECVD Al_2O_3 and SiN_x:H. Screen printing in combination with laser fired contacts (LFC) is applied to contact the front and rear side. The measured open circuit voltage and efficiency of the best cell of every group is shown in Fig. 8.

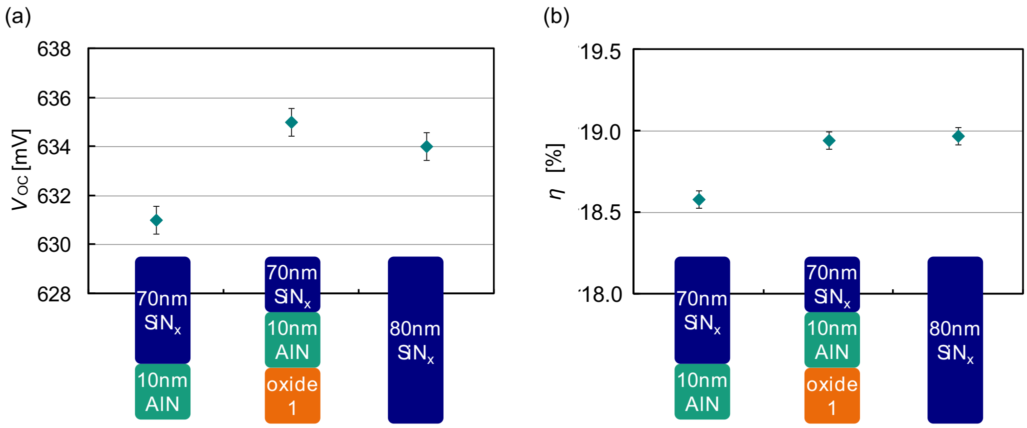

Fig. 8. Open circuit voltage and efficiency for PERC solar cells after forming gas anneal (300°C for 2 min).

The shown cell parameters indicate that the surface passivation presented on symmetrical test structures for the stack of AlN:H in combination with a thin interfacial oxide and a SiN_x:H capping layer can be transferred to cell level. Furthermore, also other relevant properties like reflectivity, absorption and firing through of the silver fingers are suited for the use as a combined anti-reflective coating and passivation layer in p-type solar cells.

Even more interesting is the application of this stack on the front of n-type solar cells where mostly Al_2O_3/SiN_x:H stacks are used at the moment. This will be analyzed in further experiments.

Due to the capability to passivate both, highly doped n-type and p-type silicon surfaces these stacks are also a promising alternative for the rear side passivation of interdigitated back contact (IBC) solar cells.

4. Conclusion

AlN:H layers have been studied with a great variety of different measurement techniques. Polycrystalline growth in the wurtzite structure with a high mass density has been presented. The influence of different deposition parameters on the interface properties is analyzed. A model for the formation of negative fixed charges inside the layers is presented based on the charge state of ionized point defect inside AlN. Additionally, stacks of AlN:H and SiN_x:H deposited on a thin low temperature interface are studied for the passivation of silicon surfaces. It is shown that the same passivation level of a 75 Ω/sq. phosphorus emitter can be reached with these stacks as with SiN_x:H.

Moreover, these stacks can lead to a similar passivation of a 70 Ω/sq. boron emitter compared to typically used Al_2O_3/SiN_x:H stacks. Obvious applications of these stacks are therefore the emitter passivation on the front of n-type solar cells and the rear passivation of IBC solar cells.

Acknowledgements

Support of Deutsche Bundesstiftung Umwelt is gratefully acknowledged.

References

[1] G. Krugel, A. Sharma, W. Wolke, J. Rentsch, und R. Preu, „Study of hydrogenated AlN as an anti-reflective coating and for the effective surface passivation of silicon“, *physica status solidi (RRL) – Rapid Research Letters*, S. n/a–n/a, 2013.

[2] G. Krugel, A. Sharma, A. Moldovan, W. Wolke, J. Rentsch, und R. Preu, „Passivation of Solar Cell Emitters Using Aluminum Nitride“, gehalten auf der 39th IEEE Photovoltaic Specialists Conference, Tampa, Florida, USA, 2013.

[3] W. Wolke, A. Jäckle, R. Preu, S. Wieder, und M. Ruske, „SiN:H anti-reflection coatings for c-Si solar cells by large scale inline sputtering“, in *Proceedings of the 19th European Photovoltaic Solar Energy Conference*, Paris, France, 2004, Bd. 1, S. 419–22.

[4] G. Krugel, W. Wolke, F. Wagner, und R. Preu, „Sputtered Aluminum Oxide for Rear Side Passivation of p-type Silicon Solar Cells“, gehalten auf der 27th European Photovoltaic Solar Energy Conference, Frankfurt, Germany, 2012.

[5] A. Moldovan, G. Krugel, F. Feldmann, M. Zimmer, J. Rentsch, und A. Roth-Fölsch, „Easy Applicable Cleaning and Conditioning of Si Surfaces with UV/Ozone Sources“, gehalten auf der 4th SiliconPV, 's-Hertogenbosch, The Netherlands, 2014.

[6] C. Ozgit, I. Donmez, M. Alevli, und N. Biyikli, „Self-limiting low-temperature growth of crystalline AlN thin films by plasma-enhanced atomic layer deposition“, *Thin Solid Films*, Bd. 520, Nr. 7, S. 2750–2755, Jan. 2012.

[7] F. Engelmark, G. Fucntes, I. V. Katardjiev, A. Harsta, U. Smith, und S. Berg, „Synthesis of highly oriented piezoelectric AlN films by reactive sputter deposition“, in *The 46th international symposium of the american vacuum society*, 2000, Bd. 18, S. 1609–1612.

[8] P. Scherrer, „Bestimmung der Größe und der inneren Struktur von Kolloidteilchen mittels Röntgenstrahlen“, *Nachrichten von der Gesellschaft der Wissenschaften zu Göttingen, Mathematisch-Physikalische Klasse*, Bd. 1918, S. 98–100.

[9] G. A. Slack und S. F. Bartram, „Thermal expansion of some diamondlike crystals“, *Journal of Applied Physics*, Bd. 46, Nr. 1, S. 89–98, 1974.

[10] T. P. Drüsedau, T. Neubert, und A. N. Panckow, „The properties of aluminum oxide and nitride films prepared by d.c. sputter-deposition from metallic targets“, *Surface and Coatings Technology*, Bd. 163–164, S. 164–168, Jan. 2003.

[11] T. P. Drüsedau und J. Bläsing, „Optical and structural properties of highly c-axis oriented aluminum nitride prepared by sputter-deposition in pure nitrogen“, *Thin Solid Films*, Bd. 377–378, S. 27–31, Dez. 2000.

[12] Y.-J. Yong, J.-Y. Lee, H. S. Kim, und J. Yong Lee, „High resolution transmission electron microscopy study on the microstructures of aluminum nitride and hydrogenated aluminum nitride films prepared by radio frequency reactive sputtering“, *Applied Physics Letters*, Bd. 71, Nr. 11, S. 1489–1491, 1997.

[13] J. C. Loretz, B. Despax, P. Marti, und A. Mazel, „Hydrogenated aluminum nitride thin films prepared by r.f. reactive sputtering. Infrared and structural properties“, *Thin Solid Films*, Bd. 265, Nr. 1–2, S. 15–21, Sep. 1995.

[14] M. Wilson, J. Lagowski, L. Jastrzebski, A. Savtchouk, und V. Faifer, „COCOS (corona oxide characterization of semiconductor) non-contact metrology for gate dielectrics“, *AIP Conference Proceedings*, Bd. 550, Nr. 1, S. 220–225, Jan. 2001.

[15] N. M. Terlinden, G. Dingemans, M. C. M. van de Sanden, und W. M. M. Kessels, „Role of field-effect on c-Si surface passivation by ultrathin (2–20 nm) atomic layer deposited Al2O3“, *Applied Physics Letters*, Bd. 96, Nr. 11, S. 112101–112101–3, März 2010.

[16] T. Mattila und R. M. Nieminen, „Point-defect complexes and broadband luminescence in GaN and AlN“, *Physical Review B*, Bd. 55, Nr. 15, S. 9571–9576, Apr. 1997.

[17] C. Stampfl und C. G. Van de Walle, „Theoretical investigation of native defects, impurities, and complexes in aluminum nitride“, *Phys. Rev. B*, Bd. 65, Nr. 15, S. 155212, Apr. 2002.

[18] R. S. Johnson, G. Lucovsky, und I. Baumvol, „Physical and electrical properties of noncrystalline Al2O3 prepared by remote plasma enhanced chemical vapor deposition“, *Journal of Vacuum Science & Technology A*, Bd. 19, Nr. 4, S. 1353–60, 2001.

[19] A. B. Sproul, „Dimensionless solution of the equation describing the effect of surface recombination on carrier decay in semiconductors“, *Journal of Applied Physics*, Bd. 76, Nr. 5, S. 2851–2854, Sep. 1994.

[20] C. Bertram, „Emitterbildung und –charakterisierung für hocheffiziente Industriesolarzellen“, Diplomarbeit, Universität Tübingen, Institut für Physik, 2009.